Wood Sci Technol (2006) 40: 308–326
DOI 10.1007/s00226-006-0067-8

ORIGINAL

Celeste Pereira · Luisa M. H. Carvalho
Carlos A. V. Costa

Modeling the continuous hot-pressing of MDF

Received: 16 October 2003 / Published online: 25 February 2006

Abstract The continuous pressing became the most important press-drying process in the manufacture of wood-based panels and a great number of manufacturers have been substituting the conventional batch process by a continuous line. One of the most important and innovative aspects is the understanding of the combined effects of physical–chemical and mechanical phenomena involved. Due to the multiplicity and interdependency of these phenomena, the development of predictive models will permit the simulation of this operation and finally a better understanding, optimization and control of the press cycle. Based on a model previously developed for batch pressing, a three-dimensional model for medium density fiberboard (MDF) continuous pressing is presented by integrating all mechanisms involved in panel formation: heat and mass transfer, chemical reaction and mechanical behavior. In this case, the description of these phenomena corresponds to the modeling of a porous and heterogeneous media in movement. The main difficulty associated to this type of problems is the choice of the reference system for the numerical solution of the equations of conservation of mass, energy and momentum. This model was used to predict the evolution of the variables related with heat and mass transfer (temperature, moisture content, gas pressure and relative humidity), as well as the variables related with mechanical behavior (pressing pressure, strain, elasticity module and density). The model performance was analyzed using the typical operating conditions for the continuous pressing of MDF by comparison of its predictions with experimental data from the literature.

List of symbols

c_p	board specific heat (J kg^{-1} K^{-1})
D_{eff}	effective diffusivity of steam in open air (m^2 s^{-1})
D_{ad}	bound water diffusivity (kg s m^{-3})

C. Pereira · L. M. H. Carvalho · C. A. V. Costa
LEPAE-Laboratory of Process, Environment and Energy Engineering,
University of Porto, Rua Roberto Frias, 4050-123 Porto, Portugal
E-mail: cpereira@inegi.up.pt
E-mail: ccosta@fe.up.pt

L. M. H. Carvalho (✉)
Department of Wood Engineering, Polytechnic Institute of Viseu,
Campus Politécnico de Repeses, 3504-510 Viseu, Portugal
E-mail: lhcarvalho@demad.estv.ipv.pt

E	Young's modulus (MPa)
$\langle E \rangle$	overall Young's modulus (MPa)
H	board moisture content (weight of water /weight of dry board)
H_i	board initial moisture content
HR	relative humidity
ΔH_r	resin polycondensation enthalpy (J kg^{-1})
k_T	thermal conductivity (W m^{-1} K^{-1})
K_g	board permeability to gas phase (m^2)
L_x	board length (m)
L_y	board width (m)
L_z	board thickness (m)
$\dot{m}$	mass of water evaporated per unit volume and time (kg s^{-1} m^{-3})
M	molecular weight (kg $kgmol^{-1}$)
N	number of volumes of control
P_g	total gas pressure (N m^{-2})
P_v	steam partial pressure (N m^{-2})
$(-r_p)$	reaction rate for resin polycondensation (s^{-1})
$(-r'_p)$	water production in resin polycondensation reaction (kg of water kg^{-1} of resin s^{-1})
t	time after press closure (s)
T	temperature (K)
v_g	velocity of gas phase (m s^{-1})
v_c	velocity of the mat passing through the press (m s^{-1})
y_r	resin content (weight of resin/dry-fiber weight)
x	spatial variable (distance along x coordinate) (m)
y	spatial variable (distance along y coordinate) (m)
z	spatial variable (distance along z coordinate) (m)

Greek symbols

ε_p	board porosity (m^3 mat void/m^3 dry mat)
γ	strain
α	adhesive degree of cure
λ	heat of vaporization of water (J kg^{-1})
μ	viscous component (Pa s)
$\langle \mu \rangle$	overall viscous component (Pa s)
μ_g	gas viscosity (N s m^{-2})
μ_{ad}	chemical potential (J kg^{-1})
ρ	density (kg m^{-3})
σ	compression stress (MPa)
φ_T	flux of heat (J m^{-2} s^{-1})
φ	flux of mas (kg m^{-2} s^{-1})
τ	press cycle time (s)
ΔH_{ad}	heat of sorption (J kg^{-1})
ΔH_r	heat of reaction (J kg^{-1})

Subscripts

a	ambient
c	composite

ed	elastic-delayed
g	gas
o	reference or initial
p	platen
r	resin
s	solid
sat	saturated conditions
T	overall (mechanical component)
T	thermal (heat and mass transfer component)
v	viscous (mechanical component)
vd	delayed viscous (mechanical component)
x	horizontal coordinate along the length of the board (from the center of the board)
y	horizontal coordinate along the width of the board (from the center of the board)
z	vertical coordinate along the thickness of the board (from the center of the board)

Introduction

In the manufacture of medium density fiberboard (MDF), and of other wood-based panels, the wood fibers or particles mattress consolidation is achieved through a hot-pressing process. Several types of presses can be used: batch or continuous, steam injection, plate and/or radio-frequency or micro-waves heated. However, in the last decade, the continuous pressing became the most important technology and a great number of manufacturers have been substituting the conventional batch equipment, usually using a multi-opening press, by a continuous line. Various advantages of this process over the conventional one were reported: greater productivity; better conversion of raw-materials due to less resin pre-cure and less trim waste, faster adjustment of the press for the desired final product thickness with reduced losses of time and material, the ability to produce a thickness range from 2.5 to 50 mm of various lengths; less resin consumption and better manipulation of panel properties (e.g., the density profile) (Sturgeon and Law 1989).

In the MDF hot-pressing several coupled physico-chemical-mechanical phenomena are involved rendering this operation quite complex. The main mechanisms are heat and mass transfer, the polymerization of the adhesive and the rheological behavior. Due to the multiplicity and interdependency of these phenomena, the development of mathematical models that enable the simulation of this operation is of great importance, because it will potentiate the understanding of either the interactions or effects of operating variables and parameters on the product properties and consumption of energy and time. So, mathematical models are recognized as important tools for optimization, control and scheduling of the hot-pressing of wood-based panels.

Since the eighties, several models were already presented in the literature for the batch process, but they have inherent limitations as they do not include the coupling of all phenomena (Humphrey and Bolton 1989; Hata et al. 1990; Kamke and Wolcott 1991; Suo and Bowyer 1994). Recently, a combined

stochastic deterministic model was developed by Zombori (2001, 2003) to characterize the random mat formation and physical mechanisms during the hot-pressing of OSB. This model can predict the internal mat conditions and density in two board dimensions and also the cure of the adhesive, but not its influence on mat viscoelastic behavior. For MDF, Carvalho and Costa (1998) presented a three-dimensional (3D) unsteady-state model describing the heat and mass transfer. Lately, the data predicted by this model was used as input for a mechanical model (Carvalho et al. 2001) describing the viscoelastic behavior and finally all the mechanisms were integrated in a global model that also includes the resin cure (Carvalho et al. 2003).

For the continuous pressing, Thomen and Humphrey (1999, 2001, 2003) presented a model that accounts for combined heat and mass transfer, adhesive cure, mat densification and stress relaxation. The model enables the simulation of local temperature evolution, moisture content, steam and gas pressure, adhesive bond strength, density as well as overall heat and gas flow patterns. However, this model ignores the contribution of water and heat produced by the resin polycondensation reaction. The mechanical behavior was taken into account by a modified Burger model, already presented by Steffen (1996).

In the case of continuous pressing, the description of these phenomena corresponds to the modeling of a porous and heterogeneous media in movement. The main difficulty associated to this type of problems is the choice of the reference system to facilitate the numerical solution of the equations of conservation of mass, energy and momentum. Although the work on modeling of deformable porous media is very scarce, in particular for wood-based panels, this kind of problems has been approached in the wet pressing of paper (Roux and Vincent 1991; Bloch 1992). In both models, the equations were derived in a Eulerian reference system (fixed in the press), which results after spatial discretization in a set of non-linear algebraic equations. Another example of this type of moving boundary problems is the drying of shrinking porous materials (Rovedo et al. 1995).

Based on the model presented by Carvalho et al. (2003), a model for the continuous pressing was developed. This model, that integrates all mechanisms involved in the panel formation (simultaneous heat and mass transfer, chemical reaction and rheology) (Pereira 2002), is presented in this paper as well as its simulation capabilities in a fairly large range of parameters space. Considering that the previous papers are not explicit about the equations and the numerical method, we present a comprehensive description of the mechanisms involved, as well as the equations and the numerical method used for solving this problem. The equations for the conservation of energy, mass and momentum were deduced in a Eulerian reference system. The operation of a continuous press is a steady-state process. For any position in the press, the internal conditions stay constant along time. So, the local and global balances are presented in steady state.

Model development and numerical solution

The model equations were deduced in an Eulerian reference system (fixed in the press) (see Fig. 1). The mat surfaces are the upper and lower boundaries and symmetry in the thickness direction is considered. These surfaces will have the

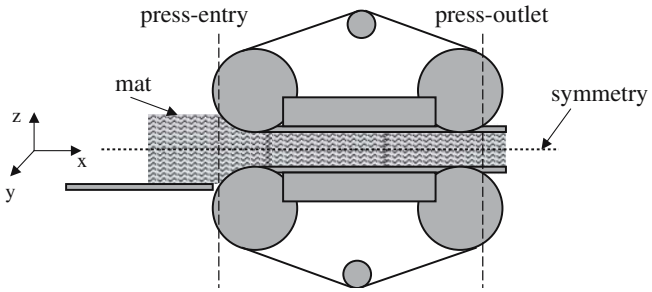

Fig. 1 Schematic of a continuous press

shape of the steel belt, i.e., its shape can be specified (position control) and the variations are related to the deformations in the mat along the press. Both surfaces in contact with the steel belt are considered closed to mass transfer. The sides of the mat and the surfaces in front and behind the press are open to heat and mass transfer with the ambient atmosphere. Another boundary condition is the temperature of the mat surfaces in contact with the steel belt. This temperature will vary along the press but it is difficult to know exactly its value and only the temperature program (temperature versus position in the feed direction) is known. We assumed that the belt does not represent any resistance to heat transfer. At inlet and outlet surfaces, as well as edges boundaries, almost all the heat transferred is due to the escape of steam and air. At these boundaries, heat transfer by conduction is neglected.

In model construction, the following assumptions were considered:

1. The model is 3D in space. Although the two surfaces in contact with the press belts can experience slightly different conditions, we assume that the center plane is a plane of symmetry (see Fig. 1). There are two planes of symmetry a horizontal mid-plane and a vertical mid-plane.
2. Two phases in thermodynamic equilibrium: solid phase (wood fibres and resin and adsorbed water) and gaseous phase (steam and air). Any resistance to heat and mass transfer between the gas phase and the adjacent solid phase is neglected. The mass of water in the adsorbed phase is neglected compared to the mass of solid (fibers and resin).
3. The total heat supplied comes from the heated press platens and from the exothermic curing reaction of the resin binder.
4. The water produced by the resin binder condensation reaction is considered.
5. The gas mixture follows the ideal gas law.
6. Physical properties in each mattress position are all temperature, moisture content and steam pressure dependent. Transport properties are dependant on physical properties changing along the board thickness.
7. The main mechanisms for heat and mass transfer are:

   - Heat is transferred by conduction due to temperature gradients and by convection due to the gas flow; conduction follows the Fourier law.
   - The gaseous phase (air + steam) is transferred by convection; each component is transferred by diffusion and convection in the whole phase. Diffusion follows the Fick law and the gas convective flow follows the Darcy law; the driving force for gas flow is the total pressure gradient and for diffusive flow is the partial pressure gradient.

- The migration of water in the adsorbed phase occurs by molecular diffusion due to the chemical potential gradient of water molecules within the adsorbed phase.
- Phase change of water from the adsorbed to the vapor state and vice versa.

8. Although it is possible to occur vitrification or plasticization of wood on the surfaces close to the platens, an additional resistance to heat and mass transfer is not considered.
9. The mattress is modeled in three dimensions although it is assumed that the consolidation of the mattress occurs only in the vertical direction and no lateral expansion is considered.
10. A perturbation in thickness (or total strain) is imposed because a position control is commonly used in industrial continuous presses.
11. Viscoelastic behavior during the whole press cycle.
12. The mechanical properties (elasticity moduli and viscous components) in each mattress position are dependant on temperature, moisture content and density of the mattress. The contribution of the resin cure reaction was not considered, as the viscous components are almost not affected by the resin cure (Carvalho et al. 2001).

In the global model, the following dependant variables were considered:

- For heat and mass transfer: temperature, gas pressure (air + steam), steam density mattress moisture content and mat density.
- For mechanical behavior: vertical position, overall compressive stress and the following set of equations.
- For heat and mass transfer: three mass balances (one for the mattress, one for the gas mixture (steam + air), and for water (adsorbed water + steam)) and one energy balance. The adsorbed water and steam are related by an equilibrium equation for the moisture sorption isotherm.
- For mechanical behavior: one equation that relates the vertical position and local strain, and the Burger model to calculate the overall stress. The top half mat is composed of Nx × Ny columns, each one with Nz layers. The strain on every control volume is calculated considering the Burger model and globally each column of Nz layers is composed by Nz Burger units in series.

For a 3D problem, the mass and energy balances in steady state are given by the following equation:

$$\text{Mat mass balance}: \quad \frac{\partial \varphi_{cx}}{\partial x} + \frac{\partial \varphi_{cy}}{\partial y} + \frac{\partial \varphi_{cz}}{\partial z} = 0 \tag{1}$$

where φ_c are the mass fluxes, ρ_c is the mat density, x, y and z are spatial variables. Relatively to the fixed reference system this mass flux is given by

$$\varphi_{ci} = v_{ci}\rho_c \quad \text{with } i = x, y \text{ and } z \tag{2}$$

where v_{ci} is the mat velocity in each direction i.

In MDF continuous pressing, the mat moves in x direction at constant velocity and mat centre (0,0,0) does not move in the directions y and z (c.f. $v_{cx} = v_{cy} = 0$). Then, the mat mass balance takes the form

$$v_{cx}\frac{\partial \rho_c}{\partial x} = 0 \tag{3}$$

$$\text{Steam mass balance}: \quad \frac{\partial \varphi_{vx}}{\partial x} + \frac{\partial \varphi_{vy}}{\partial y} + \frac{\partial \varphi_{vz}}{\partial z} - \dot{m} = 0 \tag{4}$$

where $\dot{m}$ is the mass of water evaporated per unit of volume and time.
φ_{vi} are the total steam fluxes that in a mixture are equal to (Incorpera and Witt 1990):

$$\varphi_{vi} \equiv \rho_v v_{vi} \tag{5}$$

where v_{vi} are the total steam velocities.

For a binary gas mixture in convective–diffusive flow (gaseous phase = air + steam), the steam flux relative to the mass-average velocity of the gas mixture is

$$\varphi_{vi}^{rg} = \rho_v \left(v_{vi} - v_{gi}\right) \tag{6}$$

Then, the total steam flux in the mixture is given by

$$\varphi_{vi} = \varphi_{vi}^{rg} + \rho_v v_{gi} \tag{7}$$

where v_{gi} are the gas mixture velocities andφ_{vi}^{rg} corresponds to the diffusive fluxes given by Fick's law:

$$\varphi_{vi}^{rg} = -D_{effi}\frac{\partial \rho_v}{\partial i} \tag{8}$$

where D_{effi} are the effective diffusivities of steam in air.

The mass-average velocity of the gas mixture can be expressed as a function of its relative velocity,v_{gi}^{r}, and of the mat mass-average velocity,

$$\varphi_{vi}^{rg} \equiv \rho_v \left(v_{vi} - v_{gi}\right) = \rho_v \left(v_{vi} - v_{gi}^{r} - \varepsilon_p v_{ci}\right) \tag{9}$$

The relative velocities of the gas phase in each direction are calculated using Darcy's law:

$$v_{gi}^{r} = -\frac{K_{gi}}{\mu_{gi}} \text{ grad } P_g \tag{10}$$

where K_{gi} are the board permeabilities to the gas phase,μ_{gi} the gas viscosities and P_g the total gas pressure.

Substituting Eq. 9 into Eq. 8 and$\varphi_{vi}^{r} = \varphi_{vi}^{rg} + \rho_v v_{gi}^{r}$, we obtain

$$\varphi_{vi} = \varphi_{vi}^{r} + \rho_v \varepsilon_p v_{ci} \tag{11}$$

The final form for the steam mass balance is then

$$\frac{\partial \varphi_{vx}^{r}}{\partial x} + \frac{\partial \varphi_{vy}^{r}}{\partial y} + \frac{\partial \varphi_{vz}^{r}}{\partial z} - \dot{m} + \varepsilon_p v_{cx}\frac{\partial \rho_v}{\partial x} + v_{cx}\rho_v \frac{\partial \varepsilon_p}{\partial x} = 0 \tag{12}$$

where

$$\varphi_{vi}^{r} = \rho_v v_{gi}^{r} - D_{effi}\frac{\partial \rho_v}{\partial i} \tag{13}$$

Water (adsorbed water + steam) mass balance :

$$\frac{\partial(\varphi_{\mathrm{ad}x}+\varphi_{\mathrm{v}x})}{\partial x}-\frac{\partial\left(\varphi_{\mathrm{ad}y}+\varphi_{\mathrm{v}y}\right)}{\partial y}-\frac{\partial(\varphi_{\mathrm{ad}z}+\varphi_{\mathrm{v}z})}{\partial z}=\left(-r'_{\mathrm{p}}\right)\frac{y_{\mathrm{r}}}{1+y_{\mathrm{r}}}\rho_{\mathrm{c}} \tag{14}$$

where $(-r'_{\mathrm{p}})$ is the rate of water production in the resin polycondensation reaction (Carvalho et. al. 2003), y_r is resin content.$\varphi_{\mathrm{ad}i}$ are the total fluxes of water in the adsorbed phase calculated using

$$\varphi_{\mathrm{ad}i}=\varphi^{\mathrm{r}}_{\mathrm{ad}i}+v_{\mathrm{c}i}\rho_{\mathrm{c}}H \tag{15}$$

where $\varphi^{\mathrm{r}}_{\mathrm{ad}i}$ are the relative fluxes of water in the adsorbed phase. Substituting into Eq. 14, the final form of the mass balance for water is

$$\frac{\partial\left(\varphi^{\mathrm{r}}_{\mathrm{ad}x}+\varphi^{\mathrm{r}}_{\mathrm{v}}\right)}{\partial x}-\frac{\partial\left(\varphi^{\mathrm{r}}_{\mathrm{ad}x}+\varphi^{\mathrm{r}}_{\mathrm{v}x}\right)}{\partial y}-\frac{\partial\left(\varphi^{\mathrm{r}}_{\mathrm{ad}x}+\varphi^{\mathrm{r}}_{\mathrm{v}x}\right)}{\partial z}=\left(-r'_{\mathrm{p}}\right)\frac{y_{\mathrm{r}}}{1+y_{\mathrm{r}}}\rho_{\mathrm{c}}-v_{\mathrm{c}x}\frac{\partial(\rho_{\mathrm{c}}H)}{\partial x}-\varepsilon_{\mathrm{p}}v_{\mathrm{c}x}\frac{\partial\rho_{\mathrm{v}}}{\partial x}-v_{\mathrm{c}x}\rho_{\mathrm{v}}\frac{\partial\varepsilon_{\mathrm{p}}}{\partial x} \tag{16}$$

where

$$\varphi^{\mathrm{r}}_{\mathrm{ad}i}=D_{\mathrm{ad}i}\left(1-\varepsilon_{\mathrm{p}}\right)\frac{\partial\mu_{\mathrm{ad}}}{\partial i} \tag{17}$$

$D_{\mathrm{ad}i}$ are the bound water diffusivities and μ_{ad} is the water chemical potential.

The water in the adsorbed phase is in equilibrium with the steam in voids and this equilibrium is described by the sorption isotherm:

$$H=f(\mathrm{HR},T)\quad\text{with HR}=\frac{\rho_{\mathrm{v}}}{\rho_{\mathrm{sat}}} \tag{18}$$

HR is the relative humidity and ρ_{sat} is the saturated steam density.

Gas mixture (air + steam) mass balance : $$\frac{\partial\varphi_{\mathrm{g}x}}{\partial x}+\frac{\partial\varphi_{\mathrm{g}y}}{\partial y}+\frac{\partial\varphi_{\mathrm{g}z}}{\partial z}-\dot{m}=0 \tag{19}$$

where $\varphi_{\mathrm{g}i}$ are the total gas fluxes given by

$$\varphi_{\mathrm{g}i}=\varphi_{\mathrm{v}i}+\varphi_{\mathrm{ar}i}=\rho_{\mathrm{g}}v_{\mathrm{g}i} \tag{20}$$

where the air fluxes$\varphi_{\mathrm{ar}i}$ have also two contributions: diffusive and convective in the gas mixture.

Assuming an ideal binary gas mixture: $\rho_{\mathrm{g}}=\rho_{\mathrm{v}}+\rho_{\mathrm{ar}}$

The velocity of the gas phase relatively to a fixed reference system outside the mat is

$$v_{\mathrm{g}i}=\left(\varepsilon_{\mathrm{p}}v_{\mathrm{c}i}+v^{\mathrm{r}}_{\mathrm{g}i}\right)\quad\text{(Bloch, 1992)} \tag{21}$$

The final form of the mass balance for the gas mixture is then

$$\frac{\partial\varphi^{\mathrm{r}}_{\mathrm{g}x}}{\partial x}+\frac{\partial\varphi^{\mathrm{r}}_{\mathrm{g}y}}{\partial y}+\frac{\partial\varphi^{\mathrm{r}}_{\mathrm{g}z}}{\partial z}-\dot{m}+v_{\mathrm{c}x}\rho_{\mathrm{g}}\frac{\partial\varepsilon_{\mathrm{p}}}{\partial x}+\varepsilon_{\mathrm{p}}v_{\mathrm{c}x}\frac{\partial\rho_{\mathrm{g}}}{\partial x}=0 \tag{22}$$

where the relative gas fluxes$\varphi^{\mathrm{r}}_{\mathrm{g}i}$ are given by

$$\varphi^{\mathrm{r}}_{\mathrm{g}i}=-\rho_{\mathrm{g}}v^{\mathrm{r}}_{\mathrm{g}i} \tag{23}$$

$$\text{Energy balance}: \quad \frac{\partial \varphi_{\mathrm{T}x}}{\partial x}+\frac{\partial \varphi_{\mathrm{T}y}}{\partial y}+\frac{\partial \varphi_{\mathrm{T}z}}{\partial z}+\dot{m}\Delta H_{\mathrm{ad}}+\left(-r_{\mathrm{p}}\right)\frac{y_{\mathrm{r}}}{1+y_{\mathrm{r}}}\rho_{\mathrm{c}}\Delta H_{\mathrm{r}}=0 \tag{24}$$

where ΔH_{r} is the resin polycondensation enthalpy, content and $(-r'_{\mathrm{p}})$ is the reaction rate for resin polycondensation (Carvalho et al. 2003).$\varphi_{\mathrm{T}i}$ are the heat fluxes relative to the fixed reference given by

$$\varphi_{\mathrm{T}x}=c_{\mathrm{pc}}\rho_{\mathrm{c}}v_{\mathrm{c}x}T+c_{\mathrm{pg}}\rho_{\mathrm{g}}v^{\mathrm{r}}_{\mathrm{g}x}T-k_{\mathrm{T}x}\frac{\partial T}{\partial x}=c_{\mathrm{pc}}\rho_{\mathrm{c}}v_{\mathrm{c}x}T+\varphi^{\mathrm{r}}_{\mathrm{T}x} \tag{25}$$

$$\varphi_{\mathrm{T}y}=c_{\mathrm{pg}}\rho_{\mathrm{g}}v^{\mathrm{r}}_{\mathrm{g}y}T-k_{\mathrm{T}y}\frac{\partial T}{\partial y}=\varphi^{\mathrm{r}}_{\mathrm{T}y} \tag{26}$$

$$\varphi_{\mathrm{T}z}=c_{\mathrm{pg}}\rho_{\mathrm{g}}v^{\mathrm{r}}_{\mathrm{g}z}T-k_{\mathrm{T}z}\frac{\partial T}{\partial z}=\varphi^{\mathrm{r}}_{\mathrm{T}z} \tag{27}$$

T is the temperature, c_{pc} and c_{pg} are, respectively, the mat and gas specific heat.

Boundary conditions To establish the boundary conditions, we assumed that both mat surfaces in contact with the steel belt are closed to mass transfer (gas escaping) when the mat is within the press and open to ambient atmosphere in front and behind the press. The sides of the mat are open to the ambient atmosphere. At press outlet, we took into account that the board quality specifications usually define a vertical density profile with a specific average value$\bar{\rho}_{\mathrm{cfinal}}$. For the other variables, a vertical profile is also observed and the same procedure is considered taking an average value for moisture content, temperature and gas pressure at the press end,$\bar{\rho}_{\mathrm{cfinal}}$,$\bar{H}_{\mathrm{final}}$,$\bar{T}_{\mathrm{final}}$ and$\bar{P}_{\mathrm{gfinal}}$.

$$\begin{aligned} &x=0\\ &\quad \rho_{\mathrm{c}}(0,y,z)=\rho_{\mathrm{co}}; \quad \rho_{\mathrm{v}}(0,y,z)=\rho_{\mathrm{v}}(T=T_i;H=H_i;P_{\mathrm{g}}=P_{\mathrm{a}})\\ &\quad H(0,y,z)=H_i; \quad P_{\mathrm{g}}(0,y,z)=P_{\mathrm{a}}; \quad T(0,y,z)=T_i \end{aligned} \tag{28}$$

where T_i is the temperature at press entry, H_i is the moisture content at press entry, P_{a} is the ambient pressure.

$$\begin{aligned} &x=L_x\frac{2}{L_z}\int_0^{\frac{L_z}{2}}\rho_c(L_x,y,z)\mathrm{d}z=\bar{\rho}_{\mathrm{cfinal}};\\ &\quad \rho_{\mathrm{v}}(L_x,y,z)=\rho_{\mathrm{v}}(T=\bar{T}_{\mathrm{final}};H=\bar{H}_{\mathrm{final}};P_{\mathrm{g}}=\bar{P}_{\mathrm{gfinal}})\\ &\quad \frac{2}{L_z}\int_0^{\frac{L_z}{2}}H(L_x,y,z)\mathrm{d}z=\bar{H}_{\mathrm{final}};\frac{2}{L_z}\int_0^{\frac{L_z}{2}}P_{\mathrm{g}}(L_x,y,z)dz=\bar{P}_{\mathrm{gfinal}}\\ &\quad \frac{2}{L_z}\int_0^{\frac{L_z}{2}}T(L_x,y,z)\mathrm{d}z=\bar{T}_{\mathrm{final}} \end{aligned} \tag{29}$$

$$y = 0 \quad \frac{\partial H}{\partial y}(x,0,z) = 0; \quad \frac{\partial \rho_v}{\partial y}(x,0,z) = 0$$
$$\frac{\partial P_g}{\partial y}(x,0,z) = 0; \quad \frac{\partial T}{\partial y}(x,0,z) = 0 \tag{30}$$

$$y = L_y/2 \quad H\left(x,\frac{L_y}{2},z\right) = H_i; \quad \rho_v\left(x,\frac{L_y}{2},z\right) = \rho_v\left(H = H_i; T = T_a; P_g = P_a\right)$$
$$P_g\left(x,\frac{L_y}{2},z\right) = P_{ga}; \quad T\left(x,\frac{L_y}{2},z\right) = T_a \tag{31}$$

$$z = 0 \quad \frac{\partial \rho_v}{\partial z}(x,y,0) = 0; \quad \frac{\partial H}{\partial z}(x,y,0) = 0$$
$$\frac{\partial P_g}{\partial z}(x,y,0) = 0; \quad \frac{\partial T}{\partial z}(x,y,0) = 0 \tag{32}$$

$$z = L_z(x)/2 \quad \frac{\partial \rho_v}{\partial z}\left(x,y,\frac{L_z(x)}{2}\right) = 0; \quad \frac{\partial H}{\partial z}\left(x,y,\frac{L_z(x)}{2}\right) = 0$$
$$\frac{\partial P_g}{\partial z}\left(x,y,\frac{L_z(x)}{2}\right) = 0; \quad T\left(x,y,\frac{L_z(x)}{2}\right) = T_p(x) \tag{33}$$

where T_p (x) and L_z(x) are, respectively, the platen temperature and thickness programs that in steady state change along the press length.

Numerical method

This set of equations, deduced in the Eulerian reference system (press) and in steady state is a set of elliptic partial differential equations that after spatial discretization are transformed in a large set of non-linear algebraic equations. The solution of this type of problems is usually a very complicated task, considering that we have a 3D problem (slab) and the number of dependant variables is quite high. To overcome this problem, we decided to operate a change in the reference system, i.e., to use the moving mat as the reference system. Then, the problem must again be treated as an unsteady state problem and the resulting set is a pseudo-parabolic system that can be solved using the method of lines, substituting the spatial derivatives by finite differences. A different approach could be followed, namely using moving/adaptive mesh methods based on finite elements or finite differences. In the case of 3D, this is not easy to carry out successfully; very few moving mesh results for 3D problems are present in the literature (Li et al. 2002). In addition, since the final conditions are not known, an iterative method must be used to estimate them. So, using the mat as the reference system for spatial discretization, a segment of the mat with a given length is considered. The simulation will then begin when this segment enters the press and will end when it leaves the press. The advantage of a moving grid (moving reference system) versus a fixed grid (fixed reference system) is to reduce the numerical complexity of the system. However, the solution is sensitive to the length of segment and there is a problem of error propagation, mostly if the segment of the mat is too large to consider that the conditions are practically constant.

The transformation of the reference systems, from a fixed reference (in the press) (x, y, z, t) to a moving reference (x', y', z', t') in a segment of the mat (length equal to $L_{x'}$) with a velocity v_{cx} can be done as follows (Bloch 1992):

$$x' = x - v_{cx}t' \quad z' = z - v_{cz}t' = z \quad y' = y - v_{cy}t' = y \tag{34}$$

With the transformation of reference systems, the boundary conditions are also transformed. The boundary conditions $x' = 0$ and $x' = L_{x'}$ are "free" for t', and they are known only for $t' = 0$. We considered that at the mat borders in the xx's direction, the boundary conditions are equal to the segment of the mat that goes ahead for $x' = L_x$ and equal to the segment that goes behind for $x' = 0$. As some variables present a null gradient in this direction, it is reasonable to assume that at the borders, the temperature, moisture content, gas pressure and density derivatives are null. The final equations, after the change of the reference system, are implemented in dimensionless form, following the same procedure used by Carvalho et al. (2003), but their presentation is beyond the scope of this article. In the same way, the spatial variable z' that changes with time due to the deformation of the mat in the thickness direction was normalized using a transformation introduced by Landau (Landau and Lewis 1950).

The resulting unsteady-state problem was then solved using the same numerical scheme used previously for the batch process (Carvalho et al. 2002). The spatial discretization followed a finite difference scheme and the resulting set of ordinary differential equations was handled using a special stiff equations solver LSODES based on Gear method (Hindmarch 1983). The solver accepts equations in implicit form and the internal time steps are adjusted automatically. The right-hand side of the equations is calculated with a user-supplied subroutine for spatial discretization. The spatial derivatives are replaced by a three point finite difference approximation. Using the moving mat as reference, a 3D grid was laid over a segment of the mat. The spatial discretization follows the three main directions: vertical direction (thickness), transversal direction (width) and longitudinal direction (length). The discretization grid was composed by 10 points in the vertical direction (zz axis) and in the length direction (xx axis) and just 4 in the width direction (yy axis). The segment of the mat has a length of 4 m (for a press length of 28 m). After several test runs, we concluded that increasing the number of points in the direction of width to 10, the decrease of truncation error is not compensated by the substantial increase of computing time. The beginning of the simulation corresponds to the entry of a segment of the mat and the end corresponds to the exit of this segment. The time derivatives in the five partial differential equations are calculated, for each grid, sequentially. First, we calculate the global compressive stress and then the derivative of the vertical position z'. Finally, the time derivatives of temperature, steam density and total gas pressure are calculated.

Mechanical model

The overall stress σ_T and the strain $\varepsilon_{i,j,k}$ on every control volume are calculated using the integrated form Burger model:

$$\sigma_T = \frac{\varepsilon_T}{\frac{1}{\langle E \rangle} + \frac{1}{\langle E_{ed} \rangle}\left(1 - \exp\left(-\frac{\langle E_{ed} \rangle}{\eta_{vd}}\right)\right) + \frac{t}{\langle \eta_v \rangle}} \tag{35}$$

where $\langle E \rangle$ is the overall elasticity modulus, calculated from every local elasticity moduli $E_{,j,k}$, $\langle \eta_v \rangle$ is the overall viscous component calculated from every local viscous componentsη_{vij}. $\langle E_{ed} \rangle$ and $\langle \eta_{vd} \rangle$ are the elastic-delayed and viscous-delayed components (Carvalho et al. 2001).

$$\langle E \rangle = \frac{1}{N_x N_y} \sum_{ij} E_{ij} \quad E_{ij} = \frac{L_{zo}}{\Delta z_o} \frac{1}{\sum_{k=1}^{N_z} \frac{1}{E_{i,j,k}}} \tag{36}$$

$$\langle \eta_v \rangle = \frac{1}{N_x N_y} \sum_{i} \eta_{vij} \quad \frac{1}{\eta_{ij}} = \frac{\Delta z_o}{L_{zo}} \sum_{k=1}^{N_z} \frac{1}{\eta_{vi,j,k}} \tag{37}$$

$$\langle E_{ed} \rangle = \alpha_{ede} \langle E \rangle \quad \langle \eta_{vd} \rangle = \alpha_{vdv} \langle \eta_v \rangle \tag{38}$$

$$\varepsilon_{i,j,k} = \sigma_T \left[\frac{1}{E_{i,j,k}} + \frac{1}{E_{ed_{i,j,k}}} \left(1 - \exp\left(- \frac{E_{ed_{i,j,k}}}{\eta_{vd_{i,j,k}}} \right) \right) + \frac{t}{\langle \eta_{v_{i,j,k}} \rangle} \right] \tag{39}$$

Physical and transport properties

The physical, transport properties and sorption isotherms, were estimated using several correlations from literature used by Carvalho and Costa (1998), with exception for steam and bound water diffusivities and permeability. To calculate the steam effective diffusivity, an empirical tortuosity factor ζ was set as 2 in both the vertical and horizontal directions:

$$D_{eff} = \frac{\varepsilon_p^2}{\varsigma} \tag{40}$$

where D_a is the steam in air interdiffusion coefficient that was estimated using a semi-empirical equation by Stanish (1986).

The water chemical potential μ_{ad} is by definition, equal to the chemical potential of water vapor, since we assumed local thermodynamic equilibrium. From the following thermodynamic relationships

$$M_v \frac{\partial \mu_{ad}}{\partial i} = M_v \frac{\partial \mu_v}{\partial i} = -S_v \frac{\partial T}{\partial i} + V_c \frac{\partial P}{\partial i} \tag{41}$$

where M_v is the water molecular mass and S_v the entropy estimated by the following expression by Stanish (1986) for wood drying:

$$S_v = 187 + 35.1 \ln\left(\frac{T}{298.15} \right) - 8.314 \ln\left(\frac{P_v}{101325} \right) \tag{42}$$

Substituting in Eq. 17 yields

$$\varphi_{adi} = D_{ad}^T \frac{\partial T}{\partial i} + D_{ad}^P \frac{\partial P_v}{\partial i} \tag{43}$$

where the diffusivities at constant temperature D_{ad}^T and pressure D_{ad}^P are calculated using

$$D_{ad}^{T} = D_{ad}(1-\varepsilon_p)\frac{S_v}{M_v} \quad D_{ad}^{P} = D_{ad}(1-\varepsilon_p)\frac{1}{\varepsilon_p \rho_v} \tag{44}$$

In the absence of more reliable data, the bound water diffusivity was assumed to be constant and equal to the same value given by Stanish et al. (1986) for the temperature and moisture content range expected during hot-pressing:

$$D_{ad} = 3 \times 10^{-13}\,\mathrm{kg\,s\,m^{-3}} \tag{45}$$

To estimate the local elastic properties, we used the same micromechanical model PPP as Carvalho et al. (2003), that consists in three springs in series corresponding to the three elements involved (fiber + resin + gas). To account the deformation of the porous structure, the composite modulus of elasticity was calculated using a longitudinal rule of mixture combined with the relationships derived for "honeycomb" type cellular structures.

The mat permeability in the thickness and in plane directions were calculated using the following expressions (Hass 1998):

$$K_{gz} = \exp\left(\frac{1}{-0.037 + 1.1 \times 10^{-5}\rho_c - \frac{0.037}{\ln(\rho_c)}}\right) \tag{46}$$

$$K_{gi} = \exp\left(\frac{1}{-0.041 + 9.51 \times 10^{-6}\rho_c - \frac{0.015}{\ln(\rho_c)}}\right) \tag{47}$$

Results and discussion

Model predictions

This model was used to predict the evolution of heat and mass transfer variables (temperature, moisture content, steam pressure and gas pressure) and of the mechanical variable (mat density) at a given position in the mattress during the continuous pressing operation. Several simulations were carried out to show the ability of the model to perform well in a fairly large range of parameter values. In the first place, we present the results for a set of typical operating conditions. The operating conditions and the mat characteristics at the press entry used in simulations are presented in Table 1.

The steel belt temperature versus position in the feed direction is defined as a boundary condition. Since the steel belt and the steel rods or balls move along the press together with the mat, they will transfer the heat horizontally in the feed direction, as well as to start to heat the mat. So, it is difficult to determine the exact steel belt temperatures from known platen temperatures. This problem has already been mentioned by Thoemen and Humphrey (1999), but due to lack of reliable data we assumed the typical steel belt temperature profile presented in Fig. 2. The mat thickness variation program, along the press, used in simulations is also presented.

Figure 3 shows plots of temperature, moisture content, steam pressure and gas pressure along the press length within the central layer of the mattress and using the thickness position as a parameter. On each plot, the curves are

Table 1 Operating conditions and typical mat characteristics at the press entry used in simulations

Operating conditions	Mat characteristics at the press entry
Pressing speed: $v_{cx} = 0.129$ m s^{-1} Press length: 28 m	Temperature: $T_i = 35.8$°C Gas pressure: $P_{go} = 101.325$ kPa
Maximum temperature in the steel belt: $T_{pmax} = 195$°C	Moisture content: $H_i = 11\%$
Ambient temperature: $T_a = 25$°C Ambient pressure: $P_a = 101.325$ kPa	Density: $\rho_{co} = 300$ kg m^{-3} Thickness: $L_{z'o} = 43.4$ mm Length: $L_{x'} = 4$ m Width: $L_{y'} = 2.45$ m Resin content: $y_{rx} = 0.11$

numbered from 1-adjacent to the board mid-plane to 10-adjacent to the board surface.

In this figure, we can see the effect of the steel belt temperature program and of the compaction program on heat and mass transfer variables. In case of the temperature profile, it is observed variations in the steel belt temperatures for the surface layers, and for the central layers a delay in the temperature rise. As a consequence, the moisture content decreases more at the end of the press cycle. The decrease of mat thickness and porosity will give rise to an important increase in gas pressure at the beginning of the press cycle, as a result of a decrease in the available space. Another increase is noticed around 22 m, when the mattress is subjected to another compaction. The evolution of the steam partial pressure rise is alike to that occurred in a batch press. The values attained are relatively low. However, the differences observed between the surface and central layers are certainly a consequence of a higher drying rate at the surface. We conclude that the results predicted for temperature and gas pressure agree qualitatively with results presented in the literature (Steffen at al. 1999; Thoemen and Humphrey 1999, 2001), but the magnitude of the gas pressure values obtained are much lower.

Figure 4 displays the evolution of pressing pressure, viscous component and modulus of elasticity along the press length, at a given vertical position in the mattress, as well as the density profiles. The model performance was examined, imposing a perturbation in board thickness presented in plot a. The response in compressive stress is very fast and the maximum is attained around 3 m from press entry. Another peak is noticed close to the press end. In modulus of elasticity plot, an abrupt increase is also observed in the second compression of the mat. This second compaction does not affect the viscous component, because this property depends on temperature and the polymerization reaction (Carvalho et al. 2001), that are not affected.

Comparison with results from the literature

These results should be considered qualitative rather than quantitative since the estimation of many of the physical and mechanical parameters was done using correlations developed under different conditions specially, the temperature range and the materials involved (wood, particleboard, etc.)

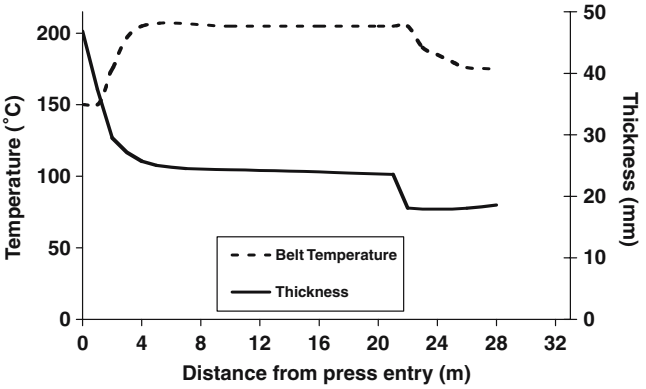

Fig. 2 Steel belt temperature and mat thickness variation program along the press

(Carvalho and Costa 1998). On the other hand, the qualitative performance of the model is difficult to evaluate because the available experimental data is scarce and the operating conditions are in most cases not completely given. Nevertheless, we show next a comparison between the model predictions and a few raw industrial data from the literature (Steffen et al. 1999). The operating conditions and the mat characteristics at the press entry used in simulations are presented in Table 2.

Figure 5 shows the experimental and simulated evolution of the temperature at the center of the board, along the length of the press. These experimental

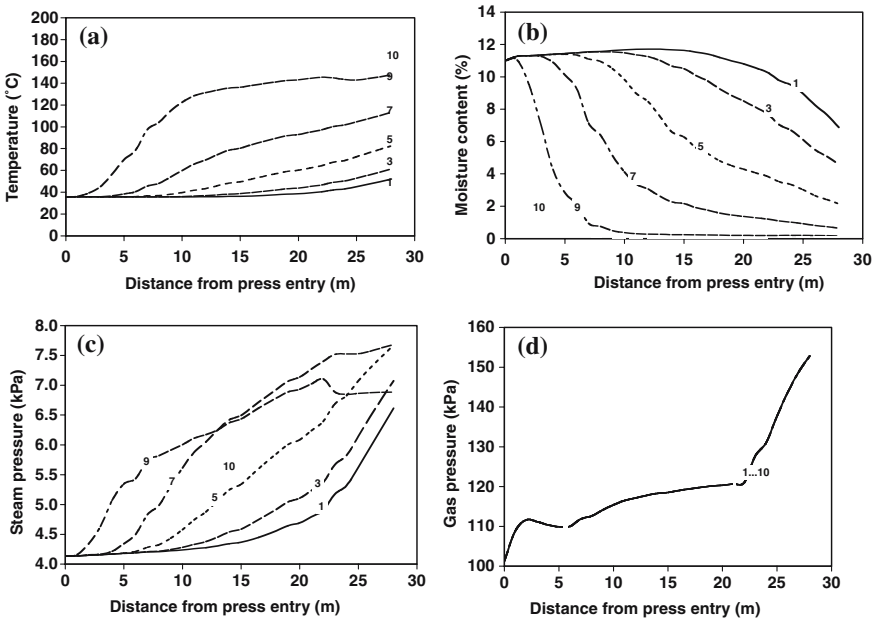

Fig. 3 Evolution of predicted **a** temperature, **b** moisture content, **c** steam partial pressure and **d** gas pressure along the press length at the central horizontal plane of the board for several positions in the vertical direction, numbered from 1 (adjacent to board mid-plane) to 10 (adjacent to board surface)

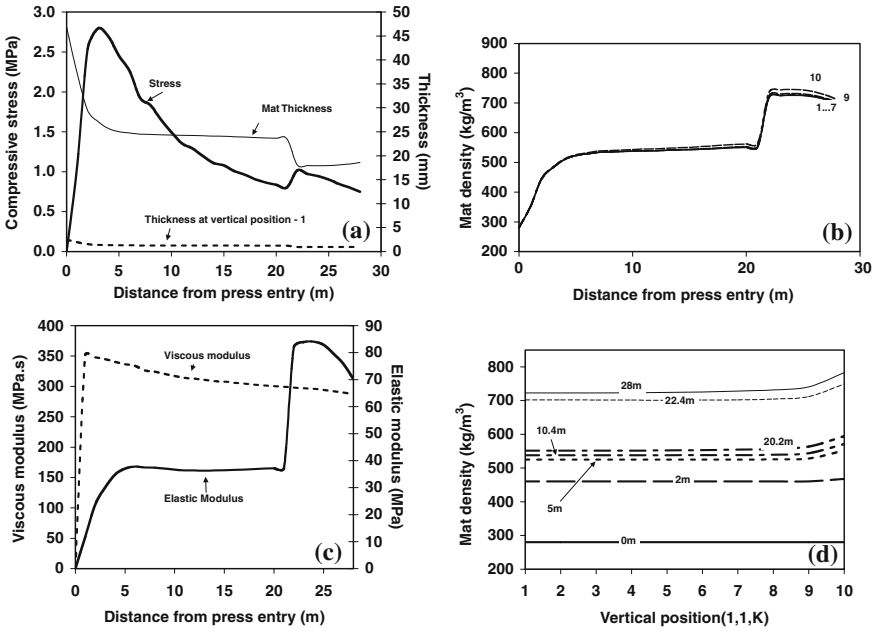

Fig. 4 Evolution of: **a** overall compressive stress **b** Young's modulus and **c** viscous component along the press length for several positions in the vertical direction (numbered from 1-adjacent to board mid-plane to 10-adjacent to board surface); **d** vertical profiles of density, along the *zz* axis, at the board mid-plane for different positions along the press length

results were obtained using thermocouples positioned near the surface and at the board center of industrial mats. As we can see, the theoretical results closely follow the experimental results at the mat surface. However, in the middle of the mat the predicted values are lower than the experimental ones. On the other hand, predicted temperature distributions obtained by Thoemen and Humphrey (2003) agree well with those measured in the industrial continuous press even for the core.

Table 2 Operating conditions and typical mat characteristics at the press entry used in simulations for comparison with the experimental results

Operating conditions	Mat characteristics at the press entry
Pressing speed: $v_{cx} = 0.129$ m s^{-1}	Temperature: $T_i = 40$°C
Press length: 28 m	Gas pressure: $P_{go} = 101.325$ kPa
Maximum temperature in the steel belt: $T_{pmax} = 215$°C	Moisture content: $H_i = 9.8\%$
Ambient temperature: $T_a = 25$°C	Density: $\rho_{co} = 280$ kg m^{-3}
Ambient pressure: $P_a = 101.325$ kPa	Thickness: $L_{z'o} = 43.4$ mm Length: $L_{x'} = 4$ m Width: $L_{y'} = 2.45$ m Resin content: $y_{rx} = 0.085$

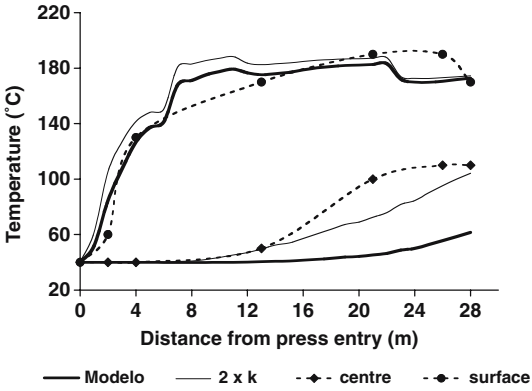

Fig. 5 Comparison between the predicted (by the model) and observed (in an industrial press from Steffen et al. 1999) results for the temperature evolution along the press length, considering two board thermal conductivities

In Fig. 6, we present the comparison between the predicted and experimental results for the evolution of gas pressure along the press length. The measurements of gas pressure were done in the board centre. This plot shows that the theoretical and experimental results are very different in magnitude. We observe a fast increase in the gas pressure near the entry, as well as, in the industrial press, but this increase has not of the same magnitude. Another increase is observed, when the mat starts to attain 100°C in the centre. The experimental value of gas pressure measured at the press outlet is near the atmospheric pressure, what probably means that this value was collected outside the press.

Several factors can originate the discrepancy between the experimental and predicted results, namely the value of some physical parameters that were calculated using correlations for wood or particleboard. It is the case of the thermal conductivity that was estimated using an empirical correlation for particleboard (Carvalho and Costa 1998). A sensitivity analysis with the global model, for the batch pressing, concluded that this property was of great importance and it was underestimated (Carvalho and Costa 2003). For the continuous press, it was verified that multiplying the thermal conductivity by a

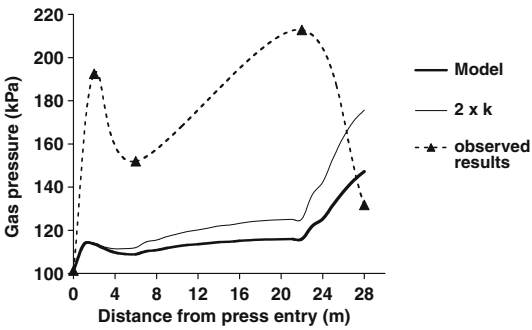

Fig. 6 Comparison between the predicted (by the model) and observed (in an industrial press from Steffen et al. 1999) results for the gas pressure evolution along the press length, considering two board thermal conductivities

factor of 2, the heating rate is higher and the results become very close, mostly at the mat center (see Fig. 5). However, for the gas pressure the model could not predict its evolution along the press, even considering a higher conductivity. So, certainly another factor is responsible for these differences between experimental and observed results. With a higher conductivity the generation of vapor increases, leading to an increase in gas pressure that is more marked in the second densification step near the end of the press, when, probably, the heat available to evaporate the moisture is larger causing a maximum in the final gas pressure. Simulation results obtained by Thoemen and Humphrey (2003) seemed to be supported by the measurements made by Steffen et al. (1999), even the predicted gas pressure maximum attained during the second densification. However, the experimental results in the industrial press were obtained by the same research group, though the pressing conditions and mat characteristics were perfectly known by these authors.

Conclusions

This paper presents a 3D model for the continuous pressing of MDF that integrates all mechanisms involved in the panel formation: heat and mass transfer, chemical reaction and mechanical behavior. This model was used to predict the evolution of the variables relating to heat and mass transfer (temperature, moisture content, gas pressure and relative humidity), as well as the variables relating to mechanical behavior (pressing pressure, strain, modulus of elasticity and density). The model performance was analyzed using the typical operating conditions for the continuous pressing of MDF and the parameters (physical, mechanical and transport properties) were calculated using the empirical and theoretical correlations from literature obtained for wood, particleboard or MDF. We observed that, in qualitative terms, the obtained results approximate those presented in the literature.

A validation of this model was attempted, using experimental data from the literature obtained in a continuous industrial press. The available data permitted to analyze the evolution of two dependant variables: temperature and gas pressure. The predicted and the experimental results were different in magnitude. Several factors can originate the discrepancy, namely the value of some physical parameters that were calculated using correlations for wood or particleboard. A sensitivity study was carried out and it was concluded that if we take a higher value for the thermal conductivity, the model can predict in an acceptable way the evolution of temperature at the board center during the press cycle, as it was already verified with a global model developed for the batch hot-pressing process of MDF.

Acknowledgements This work was done under PRAXIS XXI research project number 2/2.1/TPAR/2079/95 that is acknowledged.

References

Bloch JF (1992) Transferts de Masse et de Chaleur dans les Milieux Poreux deformables Non Satures: application au Pressage du Papier, Thèse Doctorat, Institut National Polytechnique de Grenoble, Grenoble, France

Carvalho LM, Costa C (1998) Modeling and simulation of the hot-pressing process in the production of medium density fiberboard (MDF) Chem Eng Comm 170:1–21
Carvalho LH, Costa MRN, Costa CAV (2001) Modeling rheology in the hot-pressing of MDF: comparison of mechanical models. Wood Fiber Sci 33:395–411
Carvalho LH, Costa MRN, Costa CAV (2003) A global model for the hot-pressing of MDF. Wood Sci Technol 37:241–258
Hass G (1998) Untersuchungen zur Heißpressung von Holzwerkstoffmatten unter besonderer Berücksichtigung der Verdichtung. Wood Sci Technol 24:65
Hata T, Kawai S, Sasaki H (1990) Computer simulation of temperature behavior in particle mat during hotpressing and steam injection pressing. Wood Sci Technol 24:65
Hindmarsh AC (1983) ODEPACK, a systematized collection of ODE solvers in scientific computing. In: Stepleman RS et al (eds) North Holland, New York, pp 55–64
Humphrey P, Bolton AJ (1989) The hot pressing of dry formed wood-based composites-Part II: Simulation model for heat and moisture transfer, and typical results. Holzforschung 43(3):199
Incorpera FP, Witt DP (1990) Fundamentals of heat and mass transfer. Wiley, New York
Kamke FA, Wolcott MP (1991) Fundamentals of flakeboard manufacture: wood–moisture relationships. Wood Sci Technol 25:57
Landau HG, Lewis RW (1950) Heat conduction in a melting solid. Q Appl Math 8:81–94
Li R, Tang T, Zhang P (2002) A moving mesh finite element algorithm for singular problems in two and three space dimensions. J Comput Phys 177:365–393
Pereira C (2002) Estudos da Operação de Prensagem e Cura do Aglomerado de Fibras de Media Densidade. PhD thesis, Faculdade de Engenharia da Universidade do Porto, Porto, Portugal
Roux JC, Vincent JP (1991) A proposed model analysis of wet pressing. Tappi J 189–196
Rovedo CO, Suarez C, Viollaz PE (1995) Drying Simulation of a solid slab with three-dimensional shrinkage. Drying Technol 13:371–393
Stanish MA, Schajer GS, Kayihan F (1986) A mathematical model of drying for hygroscopic porous media. AIChE J 32:1301
Steffen A (1996) Development and status of optimisation and modeling of the hot-pressing of wood-based panels. Holz Roh Werkst 54:321–332
Steffen A, Haas G, Rapp A, Humphrey P, Thoemen H (1999) Temperature and gas pressure in MDF-mats during industrial continuous hot-pressing. Holz Roh Werkst 57:154–155
Sturgeon MG, Law ML (1989) Continuous pressing of medium density fiberboard at Nelson Pine Industries New Zealand. In: Proceedings of the third European Panel Products Symposium, Washington State University, Pullman, Washington, pp 179–185
Suo S, Bowyer JL (1994) Simulation modeling of particleboard density profile. Wood Fiber Sci 26:397
Thoemen H, Humphrey PE (2001) Hot-pressing of wood-based composites: selected aspects of physics investigated by means of simulation. In: Proceedings of fifth European Panel Products Symposium, Llandudno, North Wales, UK, pp 38–49
Thoemen H, Humprey PE (1999) The continuous pressing process for wood-based panels: an analytical model. Proceedings of the third European Panel Products Symposium, Llandudno, Wales, UK, pp 18–30
Thoemen H, Humprey PE (2003) Modeling the continuous pressing process for wood-based composites. Wood Fiber Sci 35:456–468
Zombori B (2001) Modeling the transient effects during the hot-pressing of wood-based composites. PhD thesis, Faculty of the Virginia Polytechnic Institute and State University, Blacksburg, Virginia, USA
Zombori B (2003) Simulation of the internal conditions during the hot-pressing process. Wood Fiber Sci 35:2–23